*Progress In Electromagnetics Research M, Vol. 35, 97–103, 2014*

# Adaptive Cross Approximation for Scattering by Periodic Surfaces

**Jean-René Poirier*** **and Ronan Perrussel**

**Abstract**—The adaptive cross approximation is applied to boundary element matrices coming from 2D scattering problems by an infinite periodic surface. This compression technique has the advantage to be applied before the assembly of the matrix. As a result, the computational times for both assembly and solution phases are reduced. Numerical results assess the efficacy of the method on scattering problems with several periodic surfaces.

## 1. INTRODUCTION

Many engineering applications are formulated in terms of scattering by periodic structures. This is especially true in electromagnetics, where periodicity plays an important role in the design of devices. The development of broadband absorbers, the study of sea surface scattering, the design of antenna arrays, microwave lenses, and artificial dielectric media or photonic crystals are a few examples.

For the analysis of such periodic structures, the problem is usually solved by methods such as the finite difference method, finite element method, or Boundary Element Method (BEM) often also called the Method of Moments in the electromagnetics community. Because of the computational cost of such simulations, a common simplification is to consider the periodic structures as infinite. This is particularly relevant for the BEM when an appropriate Green function enables to take into account the periodicity. However the *a priori* complexity in $\mathcal{O}(N^2)$ with $N$ the number of unknowns restricts the BEM to relatively coarse grids. A method to improve this complexity is then required.

In this work, we focus on electromagnetic scattering by rough surfaces. First we recall the studied problem and the considered BEM to solve it. A few details are then introduced concerning the matrix compression technique applied to our BEM matrices. Several numerical aspects of this technique are eventually studied on representative surfaces before conclusions and prospects.

## 2. CONTINUOUS PROBLEM AND DISCRETIZATION

We consider scattering problems by a perfectly conducting $L$-periodic surface $\Gamma$ in the $E$-polarization, i.e., $E_3$ is the only non-zero component, as shown in Figure 1. The involved boundary-value problem is then the Helmholtz equation with a Dirichlet boundary condition on $\Gamma$ and a radiation condition at infinity.

These scattering problems are then formulated as a boundary integral equation [2] with a single layer potential,

$$\int_\Gamma G(\mathbf{x},\mathbf{x}_s)j(\mathbf{x}_s)d\gamma(\mathbf{x}_s) = -E^{\text{inc}}(\mathbf{x}), \quad \forall \mathbf{x} = (x_1, x_2) \text{ on } \Gamma, \tag{1}$$

where $\Gamma$ is the boundary, $E^{\text{inc}}$ the incident electric field, $j$ the sought density current, and $G$ the Green function. Variables $\mathbf{x}$ and $\mathbf{x}_s$ represent respectively the observation point and the source. In free space, this Green function is given by

$$G(\mathbf{x},\mathbf{x}_s) = \frac{1}{4i}H_0^{(2)}(k\|\mathbf{x}-\mathbf{x}_s\|) \tag{2}$$

*Received 15 January 2014, Accepted 12 March 2014, Scheduled 14 March 2014*

* Corresponding author: Jean-René Poirier (poirier@laplace.univ-tlse.fr).
The authors are with the Université de Toulouse; INPT, UPS, CNRS; LAPLACE; ENSEEIHT, Toulouse cedex 7, France.

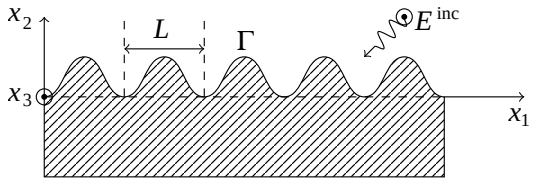


**Figure 1.** A $L$-periodic surface $\Gamma$.

where $i$ is the imaginary unit, $k$ the wave number, and $H_0^{(2)}$ the Hankel function of the second kind. This definition is replaced in the case of a periodic surface by

$$G(\mathbf{x}, \mathbf{x}_s) = \sum_{n=-\infty}^{+\infty} \frac{1}{2i\gamma_n L} e^{-i\gamma_n |x_2 - x_{s,2}|} e^{i\alpha_n (x_1 - x_{s,1})} \tag{3}$$

where $L$ is the period of the surface (see Figure 1), $\alpha_n = 2\pi n/L + k\sin(\theta)$ with $\theta$ the incident angle and $\gamma_n = \sqrt{k^2 - \alpha_n^2}$.

Note that it is not efficient to compute the sum (3) because of the slow convergence. Some improvements have been proposed to transform the sum as an integral easier to compute [2, 7].

Integral Equation (1) is then discretized using a Galerkin method with a current density constant per element. It leads to the solution of a linear system $ZI = V$ where $Z$ is a full matrix that should be compressed for memory and computational time efficiency.

## 3. MATRIX COMPRESSION

### 3.1. Hierarchical Matrix

It has been proved that some matrices issued from the BEM, as these coming from diffusion problems (electrostatics or magnetostatics), can be efficiently represented by a data-sparse format called *hierarchical matrices* and usually denoted by $\mathcal{H}$-matrices [4].

This format of matrix is based on a hierarchical matrix block partition of the original matrix. The partition of the indices of row or column can be built from the geometric positions of the degrees of freedom (dofs) of the discretization. It can be done for instance by a regular quad-tree: the dof

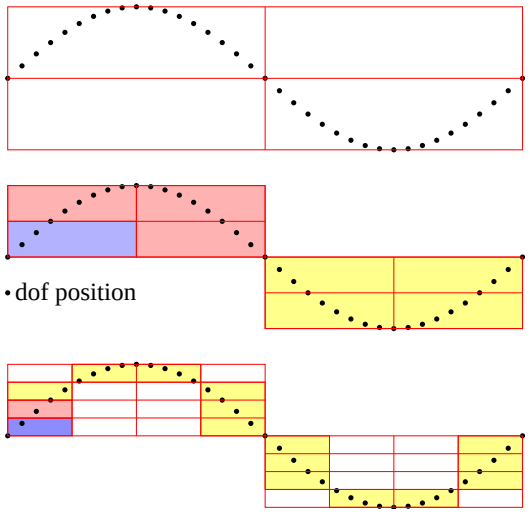


**Figure 2.** Three levels for the dof partition based on a regular quad-tree. On two levels, dofs in the blue boxes are in far-field interactions with the dofs in the yellow boxes and in near-field interactions with the dofs in the red boxes.

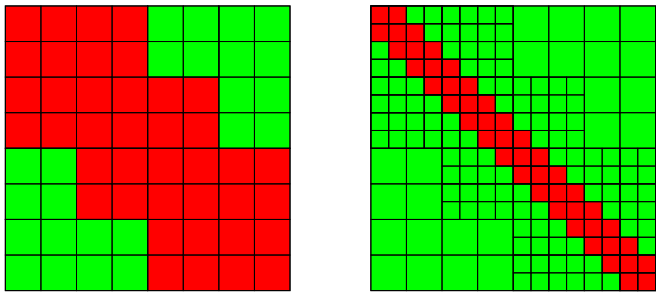

(a) (b)

**Figure 3.** Block partition of the matrix corresponding to levels 2 and 3 from Figure 2. Dofs are supposed to be numbered from left to right. Red blocks are not admissible, green ones are. First block row on each subfigure can be related to the blue boxes in Figure 2. (a) After two steps of the regular quad-tree algorithm. (b) After three steps of the regular quad-tree algorithm.

positions are enclosed in a bounding box and this box is cut in four equal boxes, this procedure is applied recursively until the number of dofs in each box is sufficiently small (see Figure 2). This regular quad-tree algorithm is the method we consider for the numerical results.

Some blocks identified, thanks to the dofs partition, satisfy an admissibility condition and can be compressed. They mainly represent far-field interactions between sets of degrees of freedom. Other non-admissible blocks have to be fully assembled and they represent near-field interactions. An example is proposed in Figure 2 to illustrate both interactions. From the dofs partition in Figure 2, the block partition of the matrix with admissible and non admissible blocks is given in Figure 3.

In order to compress the admissible blocks, several strategies can be considered as multipole expansion or panel clustering [5]. Here we prefer to focus on a purely algebraic approach, the adaptive cross approximation because it is straightforward to implement and few comparable techniques have already been considered for periodic Green's functions. For instance multipole expansion is not yet very efficient [8] for these Green functions.

### 3.2. Adaptive Cross Approximation

For the same application, a compression technique (QR algorithm) has been considered for the admissible matrix blocks in a previous work [11]. Unfortunately this method is limited by the fact that the compression is performed *a posteriori* and consequently it is necessary to assemble the whole matrix. In this work, we perform an Adaptive Cross Approximation (ACA) [1] which can be applied *a priori*. To our knowledge, this method has been applied to electromagnetic problems [6, 10], but not yet in the case of a periodic structure. It is an iterative process that computes at each iteration one row and one column (a cross) of the matrix block and an estimate of the error to approximate the block (adaptivity). More precisely, starting from a matrix block $A$ of size $L \times M$, one row and one column are computed providing two vectors respectively of size $L$ and $M$, $u_1$ and $v_1$, and the first approximate is given by $u_1 v_1^T$ ($\cdot^T$ denotes the transposition). The same operation is then applied to the residual $R = A - u_1 v_1^T$ to obtain two new vectors $u_2$ and $v_2$. By iterating this process, $A$ is approximated by $\tilde{A}_r$ a sum of $r$ rank-one updates:

$$\tilde{A}_r = \sum_{n=1}^{r} u_n v_n^T. \tag{4}$$

At each iteration we can test if

$$\|u_r\|_F \|v_r\|_F \leqslant \epsilon_{\text{ACA}} \left\|\tilde{A}_r\right\|_F, \tag{5}$$

to be able to stop the process once the required accuracy is reached; $\|\cdot\|_F$ denotes the Froebenius norm.

Note that $A$ or $R$ are never fully assembled and thus only selected entries of the matrix block have to be computed.

## 4. NUMERICAL RESULTS

The first considered problem is a surface with a sinus profile

$$x_2 = s(x_1) = h \sin\left(\frac{2\pi x_1}{L}\right) \tag{6}$$

with $h = 0.25\,\mathrm{m}$, $L = 1\,\mathrm{m}$ or a plate of the same period. Note that in the plate case, it means that $L$ is the period of the periodic Green function in the integral formulation. This plate case is only considered to validate the method on a simple example where the analytic solution is known. We also consider the scattering by a Weierstrass surface [3] described by

$$x_2 = W(x_1) = h \sum_{n=1}^{n_2} \left(\frac{1}{b^{(2-D)n}} \cos\left(\frac{2\pi b^n x_1}{L}\right)\right), \tag{7}$$

where $D$ is the fractal dimension (equal to 1.5 in our example), $n_2$ the number of scales considered, and $h$ a parameter to scale the height of this surface. The last parameter $b$ is used to characterize the lacunarity of the fractal function; it will be equal to 2 in the following experiments. Fractal surfaces have been often considered to describe rough surfaces. Among fractal surfaces, the function (7) is one of the most basic example. For a given accuracy these surfaces require more unknows than plate or sinus and may lead to a performance deterioration in terms of compression and convergence.

### 4.1. Memory Cost and Compression Rate

We first study the behavior of the compression rate: memory storage of the compressed matrix relatively to the full matrix. For the sinus profile, an example of a computation with 102400 unknowns has been considered and the corresponding memory storage is provided in Table 1. The compression rate is then simply the ratio $\dfrac{1303}{1.6\,10^5}$ given in %.

**Table 1.** Memory and computation time for a 102400-unknown problem.

| | uncompressed part | compressed part | comp. times |
|---|---|---|---|
| non admissible blocks | 389 MB | 389 MB | 11506 s |
| admissible blocks | $1.59\,10^5$ MB | 913 MB | 14385 s |
| total | $1.6\,10^5$ MB | 1303 MB | 25891 s |

The compression is studied with $\epsilon_{\mathrm{ACA}} = 10^{-8}$ and simulations are performed for several surfaces and frequencies: plate, sinus, and Weierstrass ($h = 0.25\,\mathrm{m}$) surface at 0.2 and 2 GHz. For the given ACA accuracy, the compression rate is shown in Figure 4 for an increasing number of degrees of freedom $N$.

At a given frequency, Figure 4 illustrates that the method works with the expected asymptotic behavior, i.e., an increase of the memory storage in $N\log(N)$, whatever is the block compression technique. Moreover for the same accuracy, the compression rate with the ACA decreases for an increasing frequency which is consistent with the theory. Eventually Figure 4 also shows that the geometry of the surface has an influence on the compression rate.

It is illustrated also by Figure 5 where it can be noticed that the increase of the compression rate seems roughly proportional to the frequency. It is especially noticeable in the high-frequency regime but is not always sensitive in our frequency ranges of interest.

Both assembly and solution times are shown in Figure 6. It fully justifies the use of the ACA and here again the expected asymptotic behavior is observed. Note that the full system is iteratively solved by using the Generalized minimal residual (GMRES) method [9].

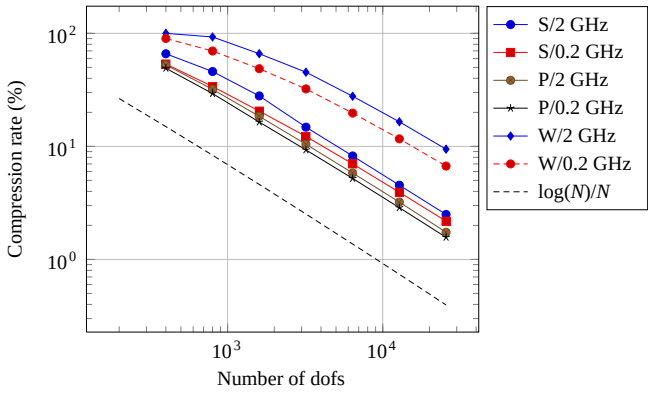


**Figure 4.** Compression rate vs the number of dofs. P: plate, S: sinus and W: Weierstrass.

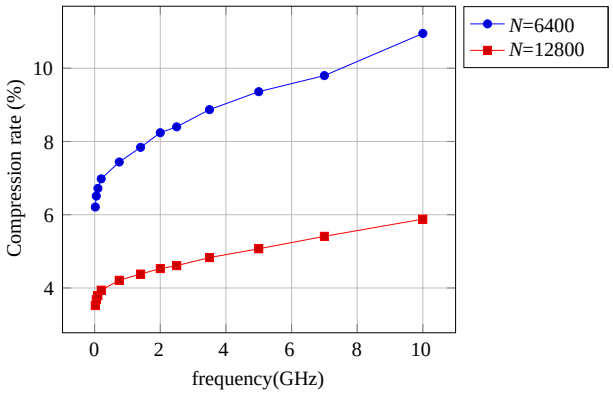


**Figure 5.** Compression rate vs the frequency.

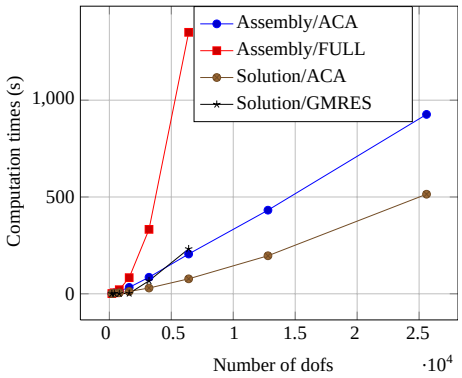


**Figure 6.** Computation times vs number of dofs.

### 4.2. Accuracy of the Solution

As no loss of accuracy can be generated by the compression technique, we have also checked the accuracy for a given solution. For this, far from the surface (i.e., $x_2 \gg \max_{x_1 \in [0,L]}(s(x_1))$), it is usual to decompose the solution to the scattering problem by a periodic surface on the basis of the outgoing Floquet modes

$$u^{\text{scat}}(x_1, x_2) = \sum_n u_n e^{i\gamma_n x_2} e^{i\alpha_n x_1}, \tag{8}$$

These modes are computed from the values of the current $j$ on the surface:

$$u_n = \frac{i}{2\gamma_n L} \int_\Gamma e^{i(\alpha_n x_1 + \gamma_n s(x_1))} j(x) d\gamma(x). \tag{9}$$

Owing to the discretization, they are directly deduced from the solution to the linear system

$$u_n = \frac{i}{2\gamma_n L} \sum_{n=1}^{N} I_n \int_{\Gamma_n} e^{i(\alpha_n x_1 + \gamma_n s(x_1))} d\gamma(x). \tag{10}$$

Figure 7 shows the convergence of the solution on the far-field, i.e., the Floquet modes. Only the propagative modes (i.e., $\gamma_n \in \mathbb{R}$), which contribute to the energy of the system, are considered. In the case of the plate, we refer to the analytic solution and in the other cases, the reference is provided by the most refined mesh. The solution error is then

$$\left( \sum_{n \in \Theta} \| u_n - u_n^{\text{ref}} \|^2 \right)^{\frac{1}{2}} \tag{11}$$

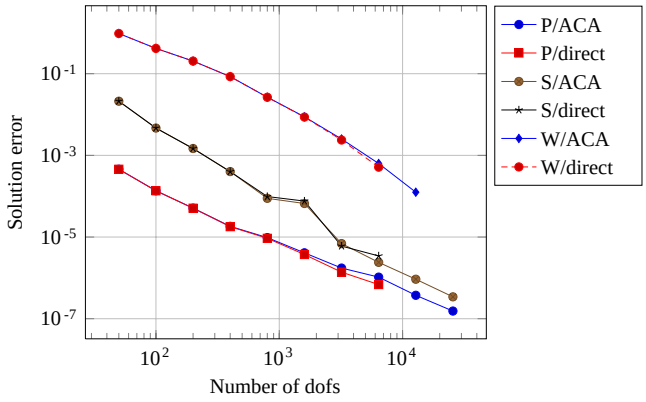


**Figure 7.** Floquet's modes convergence for several surfaces. P: plate, S: sinus and W: Weierstrass..

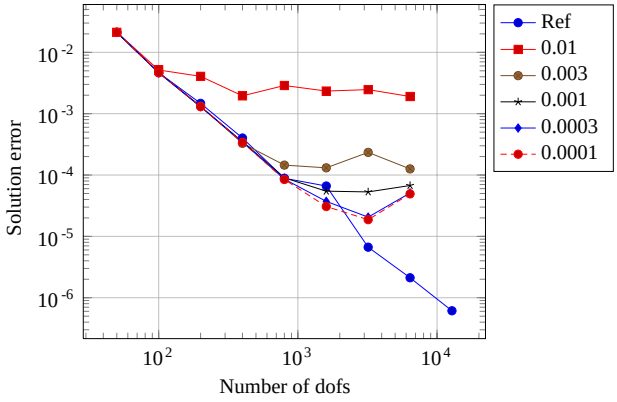


**Figure 8.** Accuracy and $\epsilon_{\text{ACA}}$.

where $\Theta$ is the set of propagative modes. In every case, the ACA solution is close to the solution provided by the direct approach and the behavior of the rate of convergence is maintained for the points computed only by the ACA method. Note that the small difference on the last point can probably be explained by the accuracy of the reference solution.

The last study concerns the choice of the parameter $\epsilon_{\text{ACA}}$. Figure 8 shows the loss of accuracy for the solution when this parameter is fixed to a given value (from 0.01 to 0.0001).

As expected for a given value of $\epsilon_{\text{ACA}}$, the computed solution differs from the direct approach when the accuracy due to the discretization is better that the accuracy of the ACA. A possible strategy in our problems is to consider $\epsilon_{\text{ACA}}$ of the form $CN^{-2}$ where $1/N$ gives roughly the mesh step and the constant $C$ can be adjusted on a coarse mesh. Thus $\epsilon_{\text{ACA}}$ is directly correlated to the accuracy of the discretization and no loss of accuracy will be due to the ACA.

## 5. CONCLUSION

As confirmed by our numerical experiments, the use of the ACA for the scattering by periodic surfaces enables to consider problems whose size cannot be accessed without compression (more than $10^5$ elements on a personal workstation). It is particularly useful when studying with a high accuracy a multiscale profile like a fractal surface. However, this kind of surface can be only treated by compression if the associated iterative method converges. As a result efficient strategies have to be implemented to be able to solve properly the resulting linear systems. This will be treated in a forthcoming work.

## REFERENCES

1. Bebendorf, M., "Approximation of boundary element matrices," *Numerische Mathematik*, Vol. 86, No. 4, 565–589, Oct. 2000.
2. DeSanto, J., G. Erdmann, W. Hereman, and M. Misra, "Theoretical and computational aspects of scattering from rough surfaces: One dimensional perfectly reecting surfaces," *Waves in Random and Complex Media*, Vol. 8, No. 4, 385–414, 1998.
3. Falconer, K., *Fractal Geometry: Mathematical Foundations and Applications,* John Wiley & Sons, 2013.
4. Hackbusch, W., "A sparse matrix arithmetic based on $\mathcal{H}$-matrices. Part I: Introduction to $\mathcal{H}$-matrices," *Computing*, Vol. 62, 89–108, 1999.
5. Hackbusch, W. and Z. P. Nowak, "On the fast matrix multiplication in the boundary element method by panel clustering," *Numerische Mathematik*, Vol. 54, 463–491, 1989.

6. Lee, J. F., K. Zhao, and M. N. Vouvakis, "The adaptive cross approximation algorithm for accelerated method of moments computations of EMC problems," *IEEE Transactions on Electromagnetic Compatibility*, Vol. 47, No. 4, 763–773, 2005.
7. Linton, C. M., "Lattice sums for the Helmholtz equation," *SIAM Review*, Vol. 52, No. 4, 630–674, 2010.
8. Otani, Y. and N. Nishimura, "A periodic FMM for Maxwell's equation in 3D and its application to problems related to photonic crystals," *Journal of Computational Physics*, Vol. 227, No. 9, 4630–4652, Feb. 2008.
9. Saad, Y. and M. H. Schultz, "GMRES: A generalized minimal residual algorithm for solving non symmetric linear systems," *SIAM J. Stat Comput.*, Vol. 7, No. 3, 856–869, Jul. 1986.
10. Stolper, M. and S. Rjasanow, "A compression method for the Helmholtz equation," *Numerical Mathematics and Advanced Applications*, 786–795, M. Feistauer, V. T. Dolej, P. Knobloch, and K. Najzar, Eds., Springer Berlin Heidelberg, 2004.
11. Tournier, S., J. Girardin, J.-R. Poirier, and P. Borderies, "Analysis of QR-compression techniques for improving electromagnetic scattering computation by periodic rough surfaces," *AMPERE, 13th International Conference on Microwave and RF Heating*, Sep. 2011.